Published in final edited form as:
J Control Release. 2011 April 10; 151(1): 28–34. doi:10.1016/j.jconrel.2011.01.008.

Positron emission tomography imaging of the stability of Cu-64 labeled dipalmitoyl and distearoyl lipids in liposomes

Jai Woong Seo[a], **Shengping Qin**[a], **Lisa M. Mahakian**[a], **Katherine D. Watson**[a], **Azadeh Kheirolomoom**[a], and **Katherine W. Ferrara**[a,*]

[a]Department of Biomedical Engineering, University of California, Davis, CA 95616, USA

Abstract

Changes in lipid acyl chain length can result in desorption of lipid from the liposomal anchorage and interaction with blood components. PET studies of the stability of such lipids have not been performed previously although such studies can map the pharmacokinetics of unstable lipids non-invasively *in vivo*. The purpose of this study was to characterize the *in vivo* clearance of ^{64}Cu-labeled distearoyl- and dipalmitoyl lipid included within long circulating liposomes. Distearoyl and dipalmitoyl maleimide lipids (1 mol%) in liposomes were labeled with a ^{64}Cu-incorporated bifunctional chelator (TETA-PDP) after the activation of pyridine disulfide to thiol by TCEP. Long circulating liposomes containing HSPC:DSPE-PEG2k-OMe:cholesterol: x (55:5:39:1), where x was ^{64}Cu-DSPE or ^{64}Cu-DPPE, or HSPC:DSPE-PEG2k-OMe:cholesterol:^{64}Cu-DSPE:DPPC (54:5:39:1:1) were evaluated in serum (*in vitro*) and via intravenous injection to FVB mice. The time activity curves for the blood, liver, and kidney were measured from PET images and the biodistribution was performed at 48 hours. *In vitro* assays showed that ^{64}Cu-DPPE transferred from liposomes to serum with a 7.9 hour half-life but ^{64}Cu-DSPE remained associated with the liposomes. The half clearance of radioactivity from the blood pool was 18 and 5 hours for ^{64}Cu-DSPE- and ^{64}Cu-DPPE liposome-injected mice, respectively. The clearance of radioactivity from the liver and kidney was significantly greater following the injection of ^{64}Cu-DPPE-labelled liposomes than ^{64}Cu-DSPE-labelled liposomes at 6, 18 and 28 hours. Forty eight hours after injection, the whole body radioactivity was 57 and 17% ID/cc for ^{64}Cu-DSPE and ^{64}Cu-DPPE, respectively. These findings suggest that the acyl chain length of the radiolabel should be considered for liposomal PET studies and that PET is an effective tool for evaluating the stability of nanoformulations in vivo.

Keywords

PET; Long circulating liposome; liposome; pharmacokinetics; bifunctional chelator; Cu-64; half clearance; liposome stability; DSPE; DPPE; lipid desorption; maleimide lipid

*To whom correspondence should be addressed: Prof. Katherine W. Ferrara, Dept. of Biomedical Engineering, 451 East Health Sciences Drive, University of California, Davis, Davis, CA 95616, PHONE: 1-530-754-9436, FAX: 1-530-754-5739, kwferrara@ucdavis.edu .
Jai Woong Seo (jwseo@ucdavis.edu)
Shengping Qin (spqin@ucdavis.edu)
Lisa M. Mahakian (lmmahakian@ucdavis.edu)
Katherine D. Watson (kdwatson@ucdavis.edu)
Azadeh Kheirolomoom (akheirolomoom@ucdavis.edu)

1. Introduction

Liposomes, spherical drug carriers composed of a lipid bilayer with a hydrophilic interior, have been investigated to improve the efficacy of drug delivery [1-5]. Long circulating liposomes in blood are achieved by incorporating polyethylene glycol (PEG) grafted lipids [6, 7] thus increasing the tumor accumulation of liposomes via the enhanced permeability and retention effect (EPR) [8]. In early studies, liposomal circulation was evaluated by inserting tritium (^{3}H, $t_{1/2}$ = 12.33 years) or carbon-14 (^{14}C, $t_{1/2}$ = 5730 years)-labeled lipids (e.g. cholesteryl hexadecyl ether (CHE)) into the lipid bilayer [9-11]. The liposomal pharmacokinetic profile in blood was measured invasively by collecting tissues from sacrificed animals [12, 13].

Advanced scintigraphic imaging techniques using gamma-radiation emitters, such as gallium-67 [14] and technetium-99m [15-18] for SPECT and fluorine-18 [19-22] and copper-64 [23, 24] for PET, facilitate tracking and quantification of liposome pharmacokinetics non-invasively. Those isotopes are encapsulated or chelated on the surface of liposomes [25]. For surface chelation, octadecylamine-diethylenetriamine pentaacetic acid (stearylamine-DTPA) [14] and dipalmitoylphosphatidylethanolamine-diethylenetriaminetetraacetic acid (DPPE-DTTA) [15, 16] have been employed as liposomal markers with Ga-67 and Tc-99m. Hydrazine nicotinamide-distearoylphhosphatidylethanolamine (HYNIC-DSPE) with Tc-99m [26] and 6-[*p*-(bromoacetamido)benzyl]-1,4,8,11-tetraazacyclotetradecane-*N*,*N*′,*N*″,*N*‴-tetraacetic acid-lipid (6-BAT lipid) with Cu-64 [23] have been developed and, in both cases, liposomal circulation and tumor accumulation were successfully measured from tomographic images. *In vivo* kinetics of new formulations must be evaluated individually and newly synthesized lipid libraries are yet to be evaluated [27]. Changes in the lipid structure, length, and head group can lead to desorption of the lipid from the liposomal anchorage and interaction with blood components [9]. The radiolabeled lipids employed in PET studies must be considered carefully as the stability of radiolabeled lipid can obfuscate image-based assessment of particle pharmacokinetics.

Recently, we developed a Cu-64 liposome labeling method using a bifunctional chelator, (6-(6-(3-(2-pyridyldithio)propionamido)hexanamido)benzyl)-1,4,8,11-tetraazacyclotetradecane-1,4,8,11-tetraacetic acid (TETA-PDP) and maleimide lipid and successfully evaluated liposomal stability using PET images (Figure 1) [28]. The ^{64}Cu-labeled bifunctional chelator was conjugated to maleimide lipids in long-circulating liposomes. In this report, this model was chosen to exemplify the differences in the rate of lipid desorption and metabolism. As defined in Table 1 and Figure 1, we examine the stability of radiolabeled lipids, 1 mol% DSPE- (two C18 acyl chains) vs 1 mol% DPPE (two C16 acyl chains)-maleimide, in long circulating liposomes which are primarily composed of HSPC (hydrogenated soy L-*α*-phosphatidylcholine), cholesterol, and DSPE-PEG2k-OMe (1,2-distearoyl-*sn*-glycero-3-phosphoethanolamine-*N*-[methoxy-(polyethyleneglycol)-2000]). In this report, substantial differences in the stability of lipids in long-circulating liposomes will be demonstrated by PET imaging.

2. Materials and methods

2.1. Materials

HSPC, DPPE-maleimide, cholesterol, DPPC and DSPE-PEG2k-OMe were purchased from Avanti Polar Lipids (Alabaster, AL) and DSPE-maleimide was purchased from NOF America Corporation (White Plains, NY). Tris(2-carboxylethyl)phosphine hydrochloride (TCEP·HCl) was purchased from Pierce (Rockford, IL). 2-Mercaptoethanol was purchased from Sigma-Aldrich (St. Louis, MO). Solvents were all of analytical purity and purchased

from Sigma-Aldrich (St. Louis, MO) and VWR (Brisbane, CA). $^{64}CuCl_2$ was purchased from Isotrace (St. Louis, MO) under a protocol controlled by the University of California, Davis. PBS was purchased from Invitrogen (Carlsbad, CA). Mouse serum was purchased from Innovative research (Novi, MI).

2.2. Preparation of maleimide liposomes

Three lipid mixtures (10 mg, Table 1) in chloroform were mixed in a test tube. Chloroform was evaporated by a gentle stream of nitrogen while vortexing. After overnight drying of the lipid film in a lyophilizer, lipids were suspended in 5 mM Alexa755 (Invitrogen, Carlsbad) solution prepared with PBS (1X, pH 7) for *in vitro* studies. For *in vivo* studies, lipids were suspended in PBS (1X, pH 7). The lipid solution was incubated at 60 °C for 5 min, drawn into the 1 mL syringe, and extruded 21 times at 60°C with 100 nm filters. Immediately after extrusion, the size was measured using a NICOMP 380 ZLS (Particle Sizing Systems, Santa Barbara, CA).

2.3. Labeling of maleimide liposomes with TETA-PDP

All labeling procedures were controlled under a protocol of the University of California, Davis. $^{64}CuCl_2$ (1 – 4.8 mCi [37 - 118 MBq]) was buffered with 0.1 M ammonium citrate (100 μL). TETA-PDP (1 mM, 2-6 μL) in an ammonium citrate buffer (0.1 M, pH 5.5), added into a $^{64}CuCl_2$ solution and chelation was performed for 40 min at 30 °C. The reaction progress was monitored by radio TLC (silica backed plate, eluent- 10% (w/w) ammonium acetate and methanol (1:1, v/v)). After the addition of excess 0.1 M tris(2-carboxylethyl)phosphine hydrochloride (TCEP·HCl) (6 μM, 60 nmol) dissolved in PBS, the solution was incubated for 5 min at room temperature. Freshly prepared maleimide liposomes (10 mg) were added to the reduced bifunctional chelator mixture. The pH was adjusted to 7 – 8 with 5.6% (v) ammonium hydroxide solution and the liposomal mixture was incubated with the activated BFC for 40 min at 30 °C. Unreacted maleimide on the surface of the liposomes was quenched by an excess (maleimide : ethanethiol = 1:10, mol/mol) of freshly prepared 0.1 M ethanethiol solution by incubating for 10 min. Non-specific binding of Cu-64 was removed by 0.1 M EDTA (20 μL), with a 5 - 10 minute incubation time. Liposomes were purified by pre-gelled size exclusion chromatography (sephadex-G75) with PBS.

2.4. *In vitro* stability test

^{64}Cu-labeled maleimide liposomes (1 mg, Table 1) prepared using the above procedure with NIR dye (Alexa 755) were added to 0.5 mL of mouse serum and volume was increased to 1 mL with PBS (1X) to create a 50% serum mixture. The mixture was incubated for 48 hours at 37°C. A portion of the liposomal serum mixture (100 μL) was hand-loaded onto a pre-conditioned sephachryl-300HR (GE Healthcare, NJ) packed column (15 mm I.D, 250 mm height) and washed with PBS. Separation was performed under 2 PSI. Eluted solution was collected into test tubes (1.5 mL/fraction), where the total eluted volume was 75 mL. The radioactivity of each fraction was measured with the 1470 Automatic Gamma Counter (Perkin-Elmer Life Sciences, MA). After the radioactive decay, the absorbance of all fractions was measured at 280 nm and fluorescence was recorded at 779 nm (ex: 755 nm). The radio TLC assay was run on aluminum-backed silica gel sheets (silica gel 60 F254, EMD, NJ), developed with chloroform/methanol/H_2O (50:40:6, v/v/v) and recorded by a radio-TLC Imaging Scanner (Bioscan, NW).

For the time-dependent liposomal stability test, the incubated liposomal serum mixture (100 μL) was collected at 0, 5, 19, 41, and 48 hours and loaded onto a pre-conditioned sephachryl-300HR (GE Healthcare, NJ) packed column (15 mm I.D, 250 mm height). Gamma counts, UV absorbance (280 nm), and fluorescence (Ex 755 nm, Em 779 nm)

measurements were gathered from each fraction. Radioactivity and fluorescence measurements were normalized by peak values.

2.5. Biodistribution study and PET scans for time-activity curves (TAC)

All animal studies were conducted under a protocol approved by the University of California, Davis Animal Care and Use Committee. A total of 16 animals (female FVB mice, 6-17 weeks, 21-39 g, Charles River, MA) were imaged over the course of this study. For each image, four or eight mice per group were anesthetized with 3.0% isofluorane and maintained at 1.5 - 2 %. ^{64}Cu-DSPE liposomes (38 ± 0.7 mg/kg, 313 ± 19 μCi [11.6 ± 0.7 MBq]/animal), ^{64}Cu-DPPE liposomes, (40 ± 6.1 mg/kg, 213 ± 112 μCi [7.88 ± 4.1 MBq]/animal), and ^{64}Cu-DSPE-1mol% DPPC liposomes (52 ± 1.2 mg/kg, 319 ± 9.1 μCi [11.8 ± 0.34 MBq]/animal) in PBS (pH 7.4) were administered to the mice by catheterized tail vein injection while on the PET scanner bed. PET imaging of ^{64}Cu-labeled liposomes was conducted with the microPET Focus (Concorde Microsystems, Inc., TN) for 30 minutes at 0, 6, 18, 28, and 48 hours after intravenous injection. Filtered backprojection (FBP) reconstruction was obtained with ASIPro software (CTI Molecular Imaging). TACs of blood, liver and kidney were obtained with region-of-interest (ROI) analysis using ASIPro software and expressed as the percentage of injected dose per cubic centimeter (%ID/cc). Whole body activity was measured in a gamma-counter (Capintec, Inc**.** NJ) and normalized by the initial value. TAC data obtained from the blood pool were fit with a one phase exponential decay ($Y=A*e^{-kt}$) generated via curve fit with Prism (GraphPad software Inc., San Diego, CA) to calculate the half clearance time.

After scanning for 48 hours, the mice were euthanized by cervical dislocation. Organs and bodily fluids of interest, such as urine, blood, spleen, lungs, diaphragm, heart, liver, kidneys, duodenum, jejunum, and quadriceps were harvested, washed with de-ionized water to remove excess blood, and weighed. Radioactivity was measured using a 1470 Automatic Gamma Counter (PerkinElmer, Inc.). Radioactivity uptake was presented as the %ID per gram of tissue. All TAC and bio-distribution data were decay corrected.

2.6 Pharmacokinetic model

Pharmacokinetic parameters were derived from our previously published pharmacokinetic model for liposomal drugs [29]. A two compartmental model for liposomes is used to calculate pharmacokinetic parameters, i.e. volume of distribution (VD), liposome elimination rate from the blood (k_{el}), liposome clearance from the blood (CL), and AUC at 24 hours for radioactivity in blood and liver. Because the lipid metabolites are eliminated quickly from the blood, without losing accuracy, we set the elimination rate of lipid metabolites from the blood to be our previously published value 0.77 h^{-1}[29]. The volume of distribution of liposomes in blood is calculated based on the mouse body weight (90 ml/kg). Vascular volume percentage in the liver is calculated based on the initial PET images and therefore the volume of distribution of liposomes in the liver is obtained. (See supplementary material)

2.7. Statistical analysis

Prism (GraphPad Software Inc., San Diego, CA) was used for statistical analysis. One-phase exponential blood clearance curves were generated via a fitted curve. The data analysis was performed using one-way analysis of variance (ANOVA) followed by Tukey's multiple comparison test.

3. Results

3.1. BFC conjugation with maleimide liposome

Liposomes (average diameter: 111 - 122 nm) were prepared using formulations defined in Table 1, as described in the experimental procedure. Copper-64 was successfully incorporated into TETA-PDP with more than 95% yield, which was confirmed by radio TLC ($^{64}CuCl_2$: R_f 0, ^{64}Cu-TETA-PDP: R_f 4.5). Treatment of ^{64}Cu-TETA-PDP by TCEP (10 equiv. TCEP over TETA-PDP) converted the disulfide to a thiol without decomplexation of Cu-64 from the chelator, which was confirmed by HPLC analysis (data not shown). The activated thiol was conjugated to maleimide lipids on the liposomal surface (pH 7.0 - 8.0); the molar ratio of the maleimide lipid was 10 times greater than ^{64}Cu-TETA-PDP. Nonspecific binding of Cu-64 was removed by EDTA and unreacted maleimide was quenched by the addition of excess mercaptoethanol. After size exclusion purification, we obtained more than 90% liposomal labeling yield. The radiochemical purity was greater than 99% on radio TLC. This method requires one hour longer than our previously reported Cu-64 liposomal surface chelation method [23]; however, the 12.7 hours half life of Cu-64 permits the use of this method and there is greater flexibility in the conjugation of the isotope to various nanoparticles with this technique.

3.2. *In vitro* stability of dual-labeled liposomes

The *in vitro* stability of three liposomal formulations was evaluated by filling the core with 5 mM of near-IR dye (Alexa Fluor750, Invitrogen Inc.) and including ^{64}Cu-DSPE, ^{64}Cu-DPPE or ^{64}Cu-DSPE-1 mol% DPPC within the liposome bilayer. After 48 hour incubation of the liposomes (each 1 mg) in PBS/mouse serum (1/1, v/v) at 37 °C and size exclusion chromatography, the fluorescence (at 789 nm), absorbance (at 280 nm) and radioactivity (gamma counter) of each fraction were measured to monitor liposomes, serum proteins, and ^{64}Cu-lipids, respectively. We collected 87 ± 1% (n = 3) of the radioactivity in 50 fractions (75 mL)(Figure 2).

For liposomes containing ^{64}Cu-DSPE or ^{64}Cu-DSPE-1 mol% DPPC, the greatest percentage of the radioactivity (91%) was collected in the liposomal fraction (fraction number 7 - 13) and in the serum fraction (fraction number 14 - 30) (Figure 2a and c) with 9%. The fluorescence in the liposomal fraction (89 - 92% intensity of total fluorescence) was similar to the radioactivity in the liposomal fraction.

Alternatively, 91% of the radioactivity in the ^{64}Cu-DPPE liposome/serum mixture was associated with the serum fraction and 7% was associated with the liposomal fraction (Figure 2b). Yet, 90% of the total fluorescence (in 50 fractions) remained associated with liposomal fraction. Thin layer chromatography (TLC) of serum fractions (fraction 17) demonstrated that the radioactivity was coincident with the liposomal fraction (fraction 11) (Figure 2, b-TLC). Radiochemical purity, measured with radio TLC, was greater than 98% for all three mixtures (^{64}Cu-DSPE and ^{64}Cu-DSPE-1 mol% DPPC liposomes in the liposomal fraction and ^{64}Cu-DPPE liposomes in the serum fraction) (Figure 2a-c TLC).

An analysis of the time-dependent liposomal stability was performed with ^{64}Cu-DPPE liposomes (1 mg) and demonstrated that the radioactivity was transferred from the liposomal fraction to the serum fraction gradually (7.9 hour half life) (Table 2). The major fluorescence peak remained in the liposomal fraction for 48 hours (Figure 3).

3.3. *In vivo* stability of ^{64}Cu-labeled liposomes

In vivo images at 0 and 18 hours after the intravenous injection of ^{64}Cu-labeled liposomes confirmed the differences in organ radioactivity between the three formulations (Figure 4).

In vivo time activity curves were then estimated (Figure 5) and fit to a single phase exponential decay curve for blood pool (Figure 5a). For ^{64}Cu-DSPE- and ^{64}Cu-DSPE-1 mol % DPPC liposomes, the percent of the injected dose per cubic centimeter within the blood pool (%ID/cc) at 0.5 hours after injection was 41 and 44 %ID/cc and at 48 hours was 8.4 and 8.2 %ID/cc, respectively. ^{64}Cu-DPPE liposomal activity decreased from 39 %ID/cc at 0.5 hours to 2.6 %ID/cc at 28 hours, significantly less than activity resulting from the injection of ^{64}Cu-DSPE-1mol% DPPC liposomes ($p<0.05$). The estimated time required for half clearance of the radioactivity was 18.5, 19.4 and 5.1 hours for ^{64}Cu-DSPE-, ^{64}Cu-DSPE-1 mol% DPPC- and ^{64}Cu-DPPE liposomes (Table 2).

Liver radioactivity was similar for the three liposomal formulations at 0.5 hour after injection (~10 %ID/cc). At later time points (6, 18, 28, and 48 hours), the accumulation of the ^{64}Cu-DSPE and ^{64}Cu-DSPE-1mol% DPPC liposomal formulations in the liver was significantly higher than ^{64}Cu-DPPE liposomes (Figure 5b). Forty eight hours after injection, the whole body radioactivity with the three liposomal formulations was 57, 55 and 17% ID/cc for ^{64}Cu-DSPE, ^{64}Cu-DSPE-1 mol% DPPC and ^{64}Cu-DPPE liposomes, respectively (Figure 5c). Radioactivity in the kidney (left kidney of prone mice) was below 10% ID/cc for all liposomes at the initial and 6 hour time points (Figure 6). Kidney activity at other time points was not measured due to the nearby activity in the liver and cecum. At 18 hours, remaining radioactivity resulting from the ^{64}Cu-DPPE liposomes was primarily observed in the intestinal track (Figure 4c, middle).

3.4. Biodistribution

At 48 hours after injection, the biodistribution of radioactivity resulting from the injection of ^{64}Cu-DSPE and ^{64}Cu-DSPE-1 mol% DPPC liposomes was similar in all organs. In each case, the highest uptake was observed in the urine, spleen and blood. Radioactivity resulting from the injection of ^{64}Cu-DPPE liposomes was below 3 %ID/g in all organs (Table 3).

4. Discussion and conclusion

Historically, lipid stability was typically determined by carbon-14, tritium or fluorescent-labeled lipids [30, 31]. Such studies demonstrated that lipid transfer or release from liposomes is associated with the degree of unsaturated acyl chains [30], liposomal size [32], temperature [33] and acyl-chain length of lipid [30]. Long circulating liposomes composed of HSPC, cholesterol, and DSPE-PEG2k-OMe, known as “Stealth liposomes”, have been optimized and extensively studied [34]. PET studies of stability have not been performed previously although such studies can map the pharmacokinetics of unstable lipids non-invasively *in vivo*. Here, we compared the PET images obtained from long circulating liposomes formulated with 1 mol% ^{64}Cu-labeled dipalmitoyl and distearoyl lipids and report the use of PET to detect the disassociation and clearance of desorbed dipalmitoyl lipid from long circulating liposomes *in vivo*.

In imaging studies using Ga-67 and Tc-99m, Hnatowich et al. previously demonstrated that radioactivity disassociated from liposomes composed of DPPC (lecithin):cholesterol: octadecylamine-DTPA (23:3:2) and that this dissociation did not result from amide-bond instability or the release of the label from the chelate [14, 35]. Ahkong et al. used dipalmitoylphosphatidylethanolamine-DTTA (DPPE-DTTA) as a Tc-99m surface chelator in DPPC liposomes (DPPC:DPPE-DTTA = 8:2 mol/mol); with their strategy, dissociation of Tc-99m from the surface of the vesicle was primarily due to non-specific binding of pertechnetate, rather than lipid exchange with plasma components or cleavage of ^{99m}Tc-DTTA from the vesicle surface [15]. However, in the Ahkong *in vitro* experiment, incubation with human plasma was evaluated for one hour. In both papers, the chelator-lipid was formulated with ~80 mol% DPPC.

Long-circulating liposomes labeled with Tc-99m have used HYNIC-DSPE in HSPC-based liposomes, and have been successfully imaged for over 24 hours *in vivo* [26]. Long circulating liposomes are often composed of 56% HSPC with a palmitoyl (C16) at the primary alcohol and a stearoyl (C18) at the secondary alcohol of glycerol. Inclusion of 39% cholesterol has been shown to stabilize liposomal structures and 5% DPSE-PEG2k-OMe increases the longevity in the blood pool (Table 1). Here, we included ^{64}Cu-TETA-PDP attached to 18 and 16 carbon chain lipids within liposomes (Figure 1). Although the head group of DSPE and DPPE maleimide lipids is quite different, as shown in Figure 1b, the circulation time in blood has been similar in previous studies using a PEG-chelator [23] and Tc-99m chelator [26] indicating that the effect of the additional cyclohexane in the head group of the maleimide lipid may be small.

Incorporation of Cu-64 in the bifunctional chelator (**1**, Figure 1) and conjugation with maleimide lipids (Figure 1b) on the surface of liposomes forms a stable covalent bond (Figure 1). Previously, the Cu-64 and TETA (benzyl-TETA) complex has been used to image the pharmacokinetics of peptides [36], antibodies [37], and nanoparticles [23]. With our labeling strategy (Figure 1), association of the radioactivity with the particle requires stable incorporation of the lipid within the liposomes. The half life of dissociation of ^{64}Cu-labeled DPPE from long circulating liposomes in serum (*in vitro*) was 7.9 hours (Table 2, Figure 3). In the blood pool (*in vivo*, Figure 5a and d), the half-clearance of ^{64}Cu-DPPE and ^{64}Cu-DSPE tracers inserted within otherwise identical liposomal formulations was 5.1 and 18.4 hours (Table 2), respectively. The greater clearance of ^{64}Cu-DPPE *in vivo* at 2.7 hours after injection, as compared with the *in vitro* disassociation of ^{64}Cu-DPPE, is likely due to disposition of liposomes to the reticuloendothelial system and resultant degradation of liposomes. This result also demonstrated that dissociated ^{64}Cu-DPPE was not circulating in blood with serum but washed out from blood pool rapidly.

Following the injection of ^{64}Cu-DPPE-labelled liposomes, TAC for liver (Figure 5b), kidney (Figure 6), and whole body radioactivity (Figure 5c) demonstrate that dissociated ^{64}Cu-DPPE radioactivity is cleared significantly faster than ^{64}Cu-DSPE. Following the injection of ^{64}Cu-DPPE liposomes, radioactivity begins to clear from the body as early as six hours after injection and activity can be visualized within the intestines (Figure 4). A biodistribution study, performed at 48 hours after injection, also showed that radioactivity in the RES following the injection of ^{64}Cu-DPPE was less than with the longer acyl chain. The results indicate that the desorbed ^{64}Cu-DPPE rapidly cleared from the blood pool and could be secreted with biliary PC through the intestine [38]. In this study, the deletion of two carbon molecules on the labeled lipid dramatically changed the PET images. *In vivo* imaging is an ideal method to detect and quantify such changes.

In order to show that the reduced circulation time for ^{64}Cu-DPPE liposomes does not result from liposome disruption caused by 1 mol% dipalmitoyl lipids, we inserted 1 mol% DPPC in liposomes that are labeled with ^{64}Cu-DSPE. The TAC data (Figure 5a) and images (Figure 4a-b, right) of ^{64}Cu-DSPE-1mol% DPPC liposomes supported the concept that the fast clearance of radioactivity was not due to the disruption of long circulating liposomes. Previously, we measured the pharmacokinetics of free Cu-64 and ^{64}Cu-labeled lipid in the blood pool, which cleared within 30 minutes [23] . Accordingly, the dissociated radiolabeled lipids are likely to clear rapidly and should not significantly hamper PET imaging of radioactivity remaining on intact particles. Blood TAC curves of ^{64}Cu-DPPE liposomes can thus reveal the dissociation rate of ^{64}Cu-DPPE when compared with stable ^{64}Cu-DSPE liposomes. Previous studies using tritium labeled DMPE-, DPPE-, DSPE-PEG2k lipids in liposomes (DSPE:cholesterol:PEG2k lipids = 50:45:5) demonstrated that DMPE- and DPPE-PEG2k are transferred from liposomes to the plasma components *in vitro* while DSPE-PEG2k remains in liposomes [9]. Although our long circulating liposomes are

primarily formulated with HSPC rather than DSPE, a similar result was obtained. Our results emphasize that the acyl chain length of the radiolabel should be considered for liposomal PET studies and that desorption can rapidly alter the apparent pharmacokinetics.

Supplementary Material

Refer to Web version on PubMed Central for supplementary material.

Acknowledgments

We thank the staff in the CMGI (Center for Molecular and Genomic Imaging, UC Davis) for assistance with ^{64}Cu and imaging studies. We appreciate the support of NIHR01CA103828 and NIHR01CA134659.

References

[1]. Medina OP, Zhu Y, Kairemo K. Targeted liposomal drug delivery in cancer. Curr. Pharm. Des. 2004; 10:2981–2989. [PubMed: 15379663]

[2]. Torchilin VP. Recent advances with liposomes as pharmaceutical carriers. Nat. Rev. Drug Discovery. 2005; 4:145–160.

[3]. Abu Lila AS, Ishida T, Kiwada H. Recent advances in tumor vasculature targeting using liposomal drug delivery systems. Expert Opin. Drug Deliv. 2009; 6:1297–1309. [PubMed: 19780711]

[4]. Abu Lila AS, Ishida T, Kiwada H. Targeting anticancer drugs to tumor vasculature using cationic liposomes. Pharm. Res. 2010; 27:1171–1183. [PubMed: 20333455]

[5]. Ferrara KW, Borden MA, Zhang H. Lipid-shelled vehicles: Engineering for ultrasound molecular imaging and drug delivery. Accounts Chem. Res. 2009; 42:881–892.

[6]. Klibanov AL, Maruyama K, Torchilin VP, Huang L. Amphipathic polyethyleneglycols effectively prolong the circulation time of liposomes. FEBS Lett. 1990; 268:235–237. [PubMed: 2384160]

[7]. Torchilin VP, Omelyanenko VG, Papisov MI, Bogdanov AA, Trubetskoy VS, Herron JN, Gentry CA. Poly(ethylene glycol) on the liposome surface - on the mechanism of polymer-coated liposome longevity. Biochim. Biophys. Acta. 1994; 1195:11–20. [PubMed: 7918551]

[8]. Gabizon A, Shmeeda H, Horowitz AT, Zalipsky S. Tumor cell targeting of liposome-entrapped drugs with phospholipid-anchored folic acid-PEG conjugates. Adv. Drug Delivery Rev. 2004; 56:1177–1192.

[9]. Li WM, Xue L, Mayer LD, Bally MB. Intermembrane transfer of polyethylene glycol-modified phosphatidylethanolamine as a means to reveal surface-associated binding ligands on liposomes. Biochim. Biophys. Acta. 2001; 1513:193–206. [PubMed: 11470091]

[10]. Dos Santos N, Allen C, Doppen AM, Anantha M, Cox KAK, Gallagher RC, Karlsson G, Edwards K, Kenner G, Samuels L, Webb MS, Bally MB. Influence of poly(ethylene glycol) grafting density and polymer length on liposomes: Relating plasma circulation lifetimes to protein binding. Biochim. Biophys. Acta. 2007; 1768:1367–1377. [PubMed: 17400180]

[11]. Pool GL, French ME, Edwards RA, Huang L, Lumb RH. Use of radiolabeled hexadecyl cholesteryl ether as a liposome marker. Lipids. 1982; 17:448–452. [PubMed: 7050582]

[12]. Semple SC, Chonn A, Cullis PR. Interactions of liposomes and lipid-based carrier systems with blood proteins: Relation to clearance behaviour in vivo. Adv. Drug Delivery Rev. 1998; 32:3–17.

[13]. Gabizon A, Shmeeda H, Barenholz Y. Pharmacokinetics of pegylated liposomal doxorubicin: Review of animal and human studies. Clin. Pharmacokinet. 2003; 42:419–436. [PubMed: 12739982]

[14]. Hnatowich DJ, Friedman B, Clancy B, Novak M. Labeling of preformed liposomes with Ga-67 and Tc-99m by chelation. J. Nucl. Med. 1981; 22:810–814. [PubMed: 7277025]

[15]. Ahkong QF, Tilcock C. Attachment of ^{99m}Tc to lipid vesicles containing the lipophilic chelate dipalmitoylphosphatidylethanolamine-DTTA. Nucl. Med. Biol. 1992; 19:831–840.

[16]. Tilcock C, Ahkong QF, Fisher D. ^{99m}Tc-labeling of lipid vesicles containing the lipophilic chelator PE-DTTA: effect of tin-to-chelate ratio, chelate content and surface polymer on labeling efficiency and biodistribution behavior. Nucl. Med. Biol. 1994; 21:89–96. [PubMed: 9234269]

[17]. Kitamura N, Shigematsu N, Nakahara T, Kanoh M, Hashimoto J, Kunieda E, Kubo A. Biodistribution of immunoliposomes labeled with Tc-99m in tumor xenografted mice. Ann. Nucl. Med. 2009; 23:149–153. [PubMed: 19225938]

[18]. Mirahmadi N, Babaei MH, Vali AM, Dadashzadeh S. Effect of liposome size on peritoneal retention and organ distribution after intraperitoneal injection in mice. Int. J. Pharm. 2010; 383:7–13. [PubMed: 19729056]

[19]. Marik J, Tartis MS, Zhang H, Fung JY, Kheirolomoom A, Sutcliffe JL, Ferrara KW. Long-circulating liposomes radiolabeled with [^{18}F]fluorodipalmitin ([^{18}F]FDP). Nucl. Med. Biol. 2007; 34:165–171. [PubMed: 17307124]

[20]. Oku N, Yamashita M, Katayama Y, Urakami T, Hatanaka K, Shimizu K, Asai T, Tsukada H, Akai S, Kanazawa H. PET imaging of brain cancer with positron emitter-labeled liposomes. Int. J. Pharm. 2011; 403:170–177. [PubMed: 20934495]

[21]. Zhang H, Kusunose J, Kheirolomoom A, Seo JW, Qi JY, Watson KD, Lindfors HA, Ruoslahti E, Sutcliffe JL, Ferrara KW. Dynamic imaging of arginine-rich heart-targeted vehicles in a mouse model. Biomaterials. 2008; 29:1976–1988. [PubMed: 18255141]

[22]. Tartis MS, Kruse DE, Zheng HR, Zhang H, Kheirolomoom A, Marik J, Ferrara KW. Dynamic microPET imaging of ultrasound contrast agents and lipid delivery. J. Control. Release. 2008; 131:160–166. [PubMed: 18718854]

[23]. Seo JW, Zhang H, Kukis DL, Meares CF, Ferrara KW. A novel method to label preformed liposomes with ^{64}Cu for positron emission tomography (PET) imaging. Bioconjugate Chem. 2008; 19:2577–2584.

[24]. Paoli EE, Kruse DE, Seo JW, Zhang H, Kheirolomoom A, Watson KD, Chiu P, Stahlberg H, Ferrara KW. An optical and microPET assessment of thermally-sensitive liposome biodistribution in the Met-1 tumor model: Importance of formulation. J. Control. Release. 2010; 143:13–22. [PubMed: 20006659]

[25]. Phillips WT, Goins BA, Bao A. Radioactive liposomes, Wiley Interdiscip. Rev.: Nanomed. Nanobiotechnol. 2009; 1:69–83.

[26]. Laverman P, Dams ET, Oyen WJ, Storm G, Koenders EB, Prevost R, van der Meer JW, Corstens FH, Boerman OC. A novel method to label liposomes with ^{99m}Tc by the hydrazino nicotinyl derivative. J. Nucl. Med. 1999; 40:192–197. [PubMed: 9935076]

[27]. Akinc A, Zumbuehl A, Goldberg M, Leshchiner ES, Busini V, Hossain N, Bacallado SA, Nguyen DN, Fuller J, Alvarez R, Borodovsky A, Borland T, Constien R, de Fougerolles A, Dorkin JR, Jayaprakash K. Narayanannair, Jayaraman M, John M, Koteliansky V, Manoharan M, Nechev L, Qin J, Racie T, Raitcheva D, Rajeev KG, Sah DW, Soutschek J, Toudjarska I, Vornlocher HP, Zimmermann TS, Langer R, Anderson DG. A combinatorial library of lipid-like materials for delivery of RNAi therapeutics. Nat. Biotechnol. 2008; 26:561–569. [PubMed: 18438401]

[28]. Seo JW, Mahakian LM, Kheirolomoom A, Zhang H, Meares CF, Ferdani R, Anderson CJ, Ferrara KW. Liposomal Cu-64 labeling method using bifunctional chelators: poly(ethylene glycol) spacer and chelator effects. Bioconjugate Chem. 2010; 21:1206–1215.

[29]. Qin SP, Seo JW, Zhang H, Qi J, Curry FRE, Ferrara KW. An Imaging-driven model for liposomal stability and circulation. Mol. Pharm. 2010; 7:12–21. [PubMed: 19621944]

[30]. Silvius JR, Leventis R. Spontaneous interbilayer transfer of phospholipids: dependence on acyl chain composition. Biochemistry. 1993; 32:13318–13326. [PubMed: 8241188]

[31]. Silvius JR, Zuckermann MJ. Interbilayer transfer of phospholipid-anchored macromolecules via monomer diffusion. Biochemistry. 1993; 32:3153–3161. [PubMed: 7681327]

[32]. Wimley WC, Thompson TE. Transbilayer and interbilayer phospholipid exchange in dimyristoylphosphatidylcholine/dimyristoylphosphatidylethanolamine large unilamellar vesicles. Biochemistry. 1991; 30:1702–1709. [PubMed: 1993185]

[33]. Jones JD, Thompson TE. Mechanism of spontaneous, concentration-dependent phospholipid transfer between bilayers. Biochemistry. 1990; 29:1593–1600. [PubMed: 2334718]

[34]. Gabizon AA. Stealth liposomes and tumor targeting: one step further in the quest for the magic bullet. Clin. Cancer Res. 2001; 7:223–225. [PubMed: 11234871]

[35]. Hnatowich DJ, Schlegel P. Albumin microspheres labeled with Ga-67 by chelation: concise communication. J. Nucl. Med. 1981; 22:623–626. [PubMed: 6788908]

[36]. Lewis JS, Srinivasan A, Schmidt MA, Anderson CJ. In vitro and in vivo evaluation of ^{64}Cu-TETA-Tyr3-octreotate. A new somatostatin analog with improved target tissue uptake. Nucl. Med. Biol. 1999; 26:267–273. [PubMed: 10363797]

[37]. Kukis DL, Diril H, Greiner DP, DeNardo SJ, DeNardo GL, Salako QA, Meares CF. A comparative study of copper-67 radiolabeling and kinetic stabilities of antibody-macrocycle chelate conjugates. Cancer. 1994; 73:779–786. [PubMed: 8306260]

[38]. Verkade HJ, Derksen JT, Gerding A, Scherphof GL, Vonk RJ, Kuipers F. Differential hepatic processing and biliary secretion of head-group and acyl chains of liposomal phosphatidylcholines. Biochem. J. 1991; 275(Pt 1):139–144. [PubMed: 2018469]

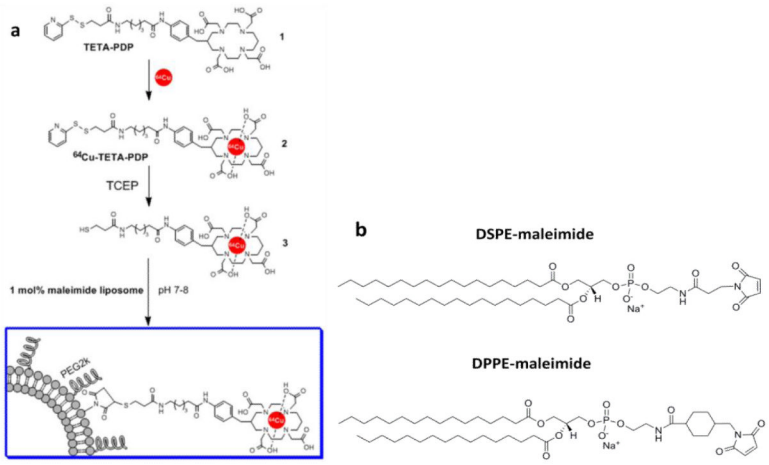

Figure 1.
a) liposomal labeling scheme using bifunctional chelator and (b) maleimide lipids exploited for ^{64}Cu-BFC conjugation

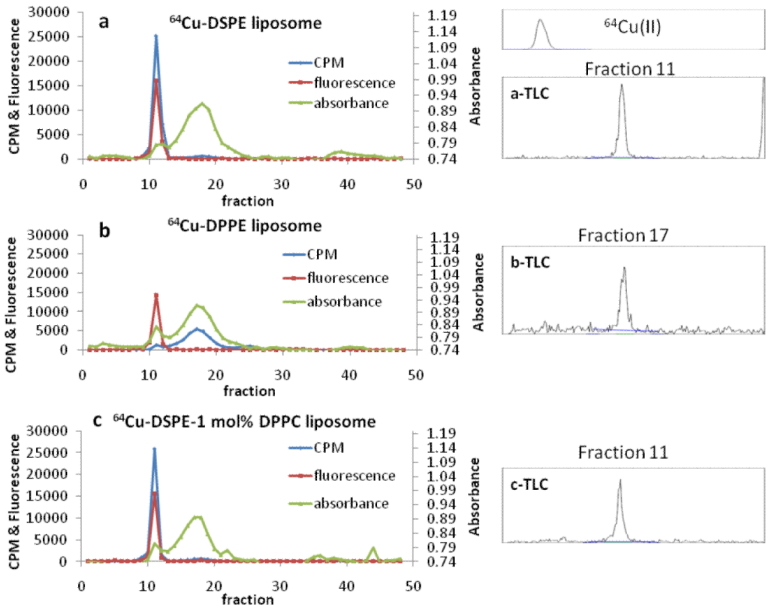

Figure 2.

In vitro stability of radio labeled lipid in three liposomes (^{64}Cu-DSPE liposomes, ^{64}Cu-DPPE liposomes, ^{64}Cu-DSPE-1mol%DPPC liposomes). Liposomes were incubated for 48 hours with 50% serum (PBS). Radio TLCs were obtained from the highest radioactive liposomal fraction (a- and c-TLC) and serum fraction (b-TLC). Blue line, CPM (counts per minute) indicates radioactivity of ^{64}Cu-lipid detected by the gamma counter. Red line represents liposomal fluorescence (779 nm). Green line, absorbance, represents serum proteins measured at 280 nm.

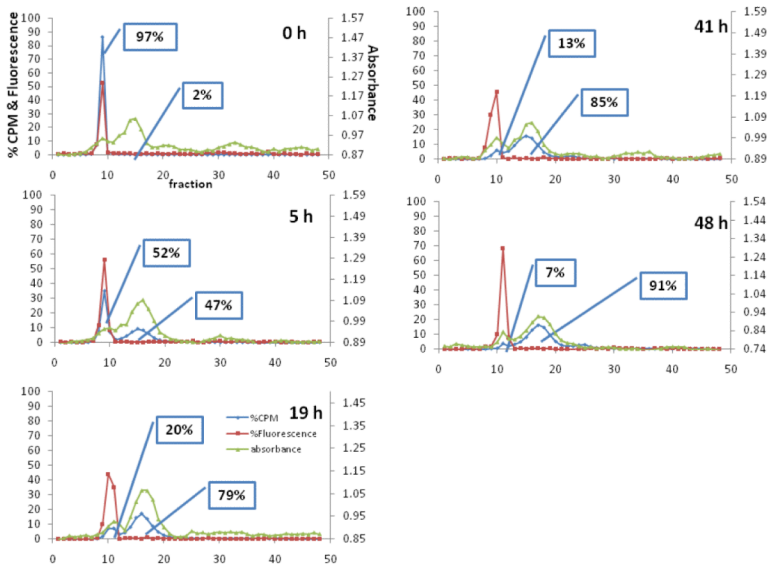

Figure 3.

Time dependent lipid transfer assay with ^{64}Cu-DPPE liposomes at 0, 5, 19, 41, and 48 hours. Blue line, CPM (counts per minute), indicates radioactivity of ^{64}Cu-lipid detected by the gamma counter. Red line represents liposomal fluorescence (779 nm). Green line, absorbance, represents serum proteins measured at 280 nm.

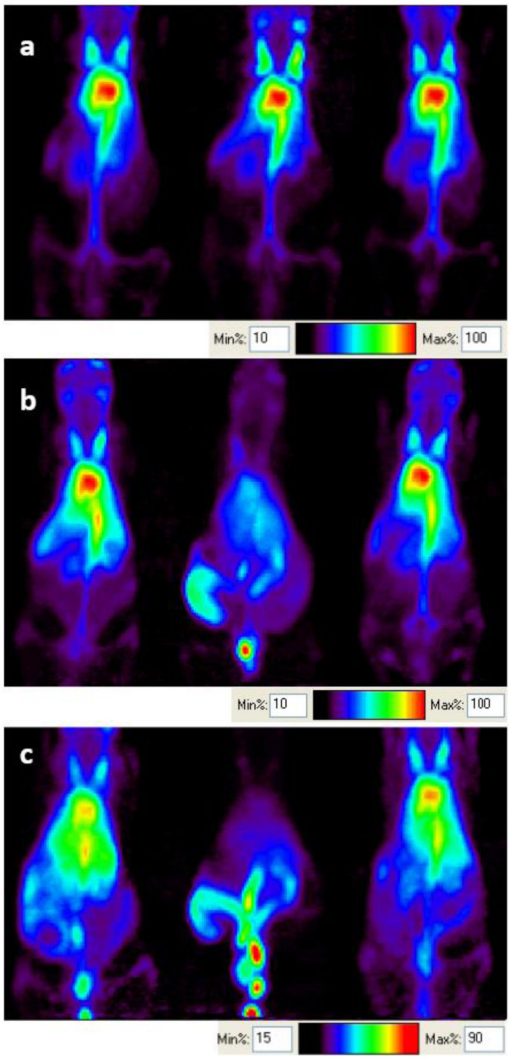

Figure 4.

a) Small-animal PET images (projected image) acquired after 30 min scanning at (a) 0, (b) 6, and (c) 18 hours. Left: ^{64}Cu-DSPE liposomes, middle: ^{64}Cu-DPPE liposomes, right: ^{64}Cu-DSPE-1mol%DPPC liposomes.

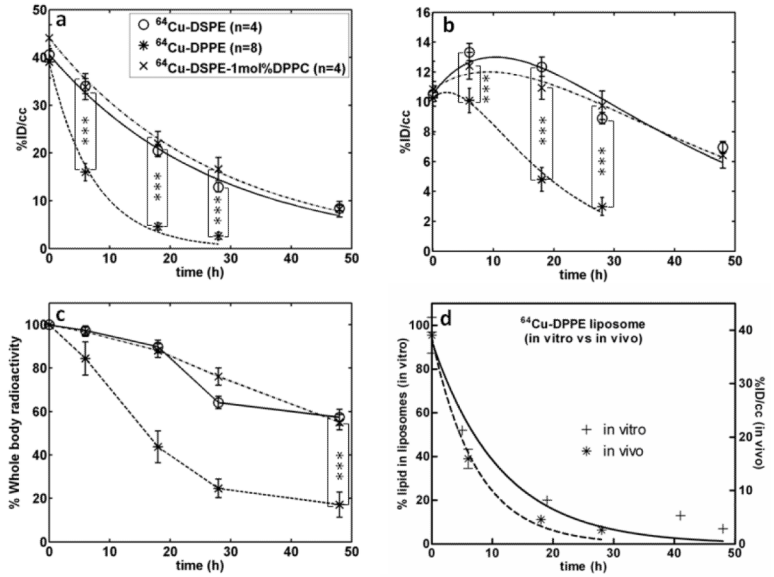

Figure 5.

Quantitative analysis (%ID/cc) of PET images with the time activity curve (TAC) of (a) blood pool and (b) liver and (c) whole body radioactivity. Three liposomes (^{64}Cu-DSPE liposomes, ^{64}Cu-DPPE liposomes, ^{64}Cu-DSPE-1mol%DPPC liposomes) were applied. (d) Comparison of stability of ^{64}Cu-DPPE liposomes from blood pool (*in vivo*) and serum incubation (*in vitro*) (curve fitted with one-phase exponential decay). Statistical analysis was performed by ANOVA, followed by Tukey's multiple comparison test (error bars, mean ± STD; ***, $P < 0.001$)

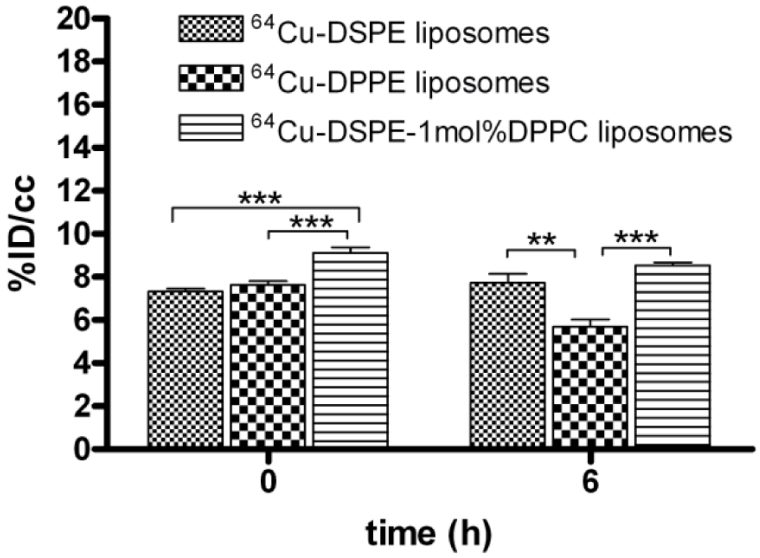

Figure 6.

Quantitative analysis (%ID/cc) of PET images of kidney. Statistical analysis was performed by ANOVA, followed by Tukey's multiple comparison test (error bars, mean ± STD; *, $P < 0.05$; **, $P < 0.01$; ***, $P < 0.001$)

Table 1

Formulations studied

Liposomes	Formulation (mol%)						Naming convention for radiolabeled liposomes
	a. HSPC	**b. DSPE-PEG2k-OMe**	**c. Cholesterol**	**d. DSPE-maleimide (MI)**	**e. DPPE-maleimide**	**f. DPPC**	
Long circulating	56	5	39	-	-	-	
1 mol% DSPE-MI[a]	55	5	39	1	-	-	^{64}Cu-DSPE liposomes
1 mol% DPPE-MI[b]	55	5	39	-	1	-	^{64}Cu-DPPE liposomes
1 mol% DSPE-MI with 1mol% DPPC[c]	54	5	39	1	-	1	^{64}Cu-DSPE-1mol% DPPC liposomes

[a] 1,2-distearoyl-*sn*-glycero-3-phosphoethanolamine-*N*-(3-maleimidopropylamide)

[b] 1,2-dipalmitoyl-*sn*-glycero-3-phosphoethanolamine-*N*-[4-(*p*-maleimidophenyl)butyramide]

[c] 1,2-dipalmitoyl-*sn*-glycero-3-phosphocholine

J Control Release. Author manuscript; available in PMC 2012 April 10.

Table 2

Pharmacokinetic parameters[a] and the half clearance time of radioactivity[b] from the blood pool in mice

Liposomes	$t_{1/2}$[c] (h)	VD[d] (mL)	AUC[e] $_{0\text{-}24h}$ (%ID/cc hr)	CL[f] (mL/h)
In vivo				
^{64}Cu-DSPE liposomes (n = 4)	18.46	3.41	646.9	0.102
^{64}Cu-DPPE liposomes (n = 8)	5.093	3.60	277.3	0.445
^{64}Cu-DSPE-1mol% DPPC liposomes (n = 4)	19.40	4.64	707.4	0.153
In vitro				
^{64}Cu-DPPE liposomes	7.857[g]	n/a	n/a	n/a

[a] pharmacokinetic parameters are derived from Figure 5a and b as described further in the supplement

[b] the half clearance times were obtained from one phase exponential decay curve fit ($Y = A\ e^{-k\times t}$).

[c] half clearance time

[d] volume of distribution

[e] area under curve at 24 hours

[f] clearance from animal

[g] half clearance was calculated based on Figure 5d (in vitro) by one-phase exponential decay curve fit ($Y = A\ e^{-k\times t}$).

Table 3

Biodistribution of ^{64}Cu-DSPE (n = 4), ^{64}Cu-DPPE (n = 8) and ^{64}Cu-DSPE-1mol% DPPC liposomes (n = 4) in mice at 48 h after injection.

Organ	^{64}Cu-DSPE (n = 4)* %ID/g ± SD	^{64}Cu-DPPE (n = 8) %ID/g ± SD	^{64}Cu-DSPE-1mol% DPPC (n = 4) %ID/g ± SD
Urine	11.93 ± 3.66	3.67 ± 1.96	13.10 ± 5.52
Blood	8.71 ± 0.38	1.51 ± 0.33	8.60 ± 1.74
Spleen	12.3 ± 0.70	1.51 ± 0.22	9.25 ± 1.28
Lungs	3.14 ± 0.25	1.03 ± 0.20	4.09 ± 0.38
Diaphragm	1.28 ± 0.16	0.49 ± 0.23	2.02 ± 0.46
Heart	2.89 ± 0.50	1.04 ± 0.12	3.41 ± 0.49
Liver	6.88 ± 0.97	2.36 ± 0.38	6.51 ± 0.58
Left kidney	6.14 ± 0.43	1.92 ± 0.25	7.56 ± 0.52
Right kidney	6.03 ± 0.52	1.90 ± 0.23	7.76 ± 0.65
Duodenum	4.83 ± 0.57	1.36 ± 0.32	5.09 ± 0.49
Jejunum	3.66 ± 0.63	1.34 ± 0.66	4.56 ± 0.58
Quadriceps	0.31 ± 0.06	0.11 ± 0.04	0.47 ± 0.04

*Data were obtained from previous report [28]